**Master of Science**

# The Functional Study of RSK4 in Human Non-small cell lung cancer

**The Graduate School**

**of the University of Ulsan**

**Department of Medical Sciences**

**Ji U Lee**

# The Functional Study of RSK4 in Human Non-small cell lung cancer

**Supervisor: Dong-Hoon Jin**

**A Dissertation**

**Submitted to**

**the Graduate School of the University of Ulsan**

**In partial Fulfillment of the Requirements**

**for the Degree of**

**Master of Science**

**by**

**Ji U Lee**

**Department of Medical Science**

**University of Ulsan, Korea**

**February 2024**

# The Functional Study of RSK4 in Human Non-small cell lung cancer

**This certifies that the dissertation of Ji U Lee is approved**

_____

**Committee Chair Dr. In Ki Kim**

_____

**Committee Member Dr. Chang Hoon Ha**

_____

**Committee Member Dr. Dong-Hoon Jin**

**Department of Medical Science**

**University of Ulsan, Korea**

**February 2024**

# ABSTRACT

The p90 ribosomal protein S6 kinase 4 (RSK4) is a serine-threonine kinase that functions downstream of the mitogen-activated protein kinase (MAPK) signaling pathway and regulates cellular processes. RSK4 was confirmed to be highly expressed in non-small cell lung cancer (NSCLC) patients with EGFR mutations through the Gene Expression Omnibus (GEO) database. The protein expression of RSK4 was upregulated in cancer tissues compared with normal tissues in patients with lung cancer. In particular, it was highly expressed NSCLC cell lines with EGFR mutations. Furthermore, when RSK4 was inhibited, apoptosis was induced only in EGFR mutation cell lines. Additionally, knockdown of RSK4 inhibited Akt phosphorylation and increased the mRNA expression of PUMA, a BH3-only protein. Interestingly, other BH3-only proteins showed no differences in expression at the mRNA and protein levels. Next, inhibition of RSK4 induced the nuclear translocation of p65, which regulates the transcription of PUMA.

In summary, these findings demonstrated that the downregulation of RSK4 inhibits the survival of cells with EGFR mutations through the Akt/p65/PUMA signaling pathway. This suggests the potential of RSK4 as a novel therapeutic target for NSCLC with EGFR mutation.

**Keyword**s: RSK4, Non-small cell lung cancer, EGFR mutation, Apoptosis, Therapeutic target

# CONTENTS

# LIST OF FIGURES

# LIST OF TABLES

# INTRODUCTION

Lung cancer is the leading cause of cancer-related deaths worldwide, with a 5-year survival rate ranging from 4 to 17%, depending on the disease stage [1-2.]. Advances in non-invasive diagnostic methods have increased the likelihood of identifying lung cancer, but only 10-15% of new cases are diagnosed at an early clinical stage [3]. Lung cancer is classified into two broad histologic categories: non-small cell lung cancer (NSCLC) and small cell lung cancer (SCLC). NSCLC accounts for 80% of all cases and is mainly classified as adenocarcinoma (LUAD), squamous cell carcinoma (LUSC), large cell lung cancer, and other variants [3-4].

NSCLC is associated with mutations in several oncogenes, such as *EGFR*, *ERBB2*, *KRAS*, and *TP53*. Among these mutations, EGFR (epidermal growth factor receptor) activating mutations occur most frequently in adenocarcinoma [5-6]. The most common EGFR mutations in NSCLC are *exon 19* deletion and *exon 21 L858R* [7-9]. Other uncommon *EGFR* mutations that can be targeted include *exon 20* alterations, insertional mutations in *exon 19*, and point mutations in *exon 18* [10]. EGFR-TKIs are targeted anticancer drug that selectively inhibits the EGFR. Thus, they are more effective and have fewer adverse effects than conventional anticancer therapies. First-generation EGFR tyrosine kinase inhibitors (TKIs) such as erlotinib and gefitinib target *exon 19* deletion and *exon 21 L858R* mutation [7-9]. A second-generation EGFR-TKI, afatinib, was designed to overcome resistance to first-generation EGFR-TKIs. Most patients develop acquired resistance through various mechanisms after 9-14 months of treatment with first- and second-generation EGFR-TKIs. The main cause of this resistance is the *T790M* mutation in *exon 20*, which is present in 50-60% of patients. Osimertinib is a third-generation EGFR-TKI designed to overcome the acquired resistance caused by the *exon 20 T790M* mutation. Currently, a fourth-generation EGFR-TKI is being investigated to overcome the *exon 20 C797S* mutation caused by third-generation EGFR-TKIs [11-12]. Since EGFR-TKIs were developed and subsequently used clinically, the survival and clinical outcomes of patients with NSCLC with EGFR mutations have improved remarkably. Thus, EGFR-TKIs are recommended as the standard first-line treatment for NSCLC patients harboring EGFR mutations. However, mutations associated with drug resistance (*exon 20 T790M*, *C797S*) have been reported in patients treated with first-generation EGFR-TKIs. These mutations induce drug resistance during treatment with the previous generations of EGFR-TKIs [13]. Therefore, in order to overcome these limitations, it is necessary to understand the signaling mechanism of EGFR mutations [14].

The p90 ribosomal protein S6 kinase (RSK) is a serine-threonine kinase that functions downstream of the Ras/Raf/MAPK/ERK pathway and regulates various cellular processes including cell migration, survival, proliferation, and growth [15-16]. This family consists of four members (RSK1 to RSK4) in humans. RSK1,2 are the most studied in cancer, and RSK3,4 have a high degree of similarity in

sequence identity in the N-terminal kinase domain (NTKD) that mediates substrate phosphorylation. Therefore, these proteins have similar biological functions [17-18]. In contrast to other RSK isoforms, RSK4 has many unique characteristics. First, the RSK1-3 expression status has been widely identified in human tissues, whereas RSK4 expressed only during embryonic development [18]. Second, RSK4 differs from the other RSKs in its activation mechanism. RSK1-3 require the activation of both ERK and phosphoinositide-dependent protein kinase 1 (PDK1) to be activated. However, RSK4 does not require PDK1 to maintain its basal activity [17]. Finally, RSK1-3 are generally present in the cytoplasm during the rest period but are known to move into the nucleus when stimulated, whereas RSK4 is mainly activated in the cytoplasm and does not accumulate in the nucleus upon stimulation [19].

RSK4 is known to be a tumor suppressor gene in endometrial cancer [20], colon cancer [21], and ovarian cancer [22], but is known to be an oncogene in kidney cancer [23], esophageal squamous cell carcinoma [24], and glioma [25]. However, the role of RSK4 in breast cancer [26-27] and lung cancers [28-29] remain controversial, and these studies suggest that the role of RSK4 in cancers remains unclear because of tissue-specific factors [30]. Therefore, it is important to study the factors and cell signaling pathways that are regulated by RSK4.

Through the GEO database, it was confirmed that RSK4 expression was increased in NSCLC patients with EGFR mutation. Additionally, the expression of RSK4 in LUAD cells induces drug resistance, tumor invasion, and metastasis, which are associated with poor patient survival [31-32]. These results suggest that RSK4 could be a therapeutic target for patients with NSCLC. Therefore, I transfected *siRSK4* in NSCLC and studied them according to their apoptotic response. Currently, the role of RSK4 in relation to EGFR mutation status has not been reported, and this study shows that RSK4 has potential as a therapeutic target in NSCLC with EGFR mutation.

# MATERIAL & METHODS

### *1. GEO database analysis*

The Gene Expression Omnibus database (GEO) is a public database for screening gene expression data, microarray data, and gene chips. In this study, I used genome expression datasets from GSE135164. The GSE135164 database contains 7 *EGFR* wild type and 4 *EGFR* mutation type patient-derived cells.

The differentially expressed genes were analyzed using GEO2R (http://www.ncbi.nlm.gov/geo2r) between *EGFR* wild type and *EGFR* mutation type samples. The significant differentially expressed genes (DEGs) were detected using the adjusted p-values and the Benjamini- Hochberg false discovery rate. The upregulated genes were identified using cut-off values of $P<0.001$ and logFC >0.

### *2. Specimens and Cell culture*

In this study, a total of seven lung cancer samples were used. I was obtained lung cancer tissues from the Bio Resource Center (BRC) of Asan Medical Center (Seoul, Republic of Korea).

H460, H292, H1299, H1650, and HCC 827 cell lines obtained from KCLB (Korea Cell Line Bank, Seoul, Korea), and the PC-9 cell line was purchased from ATCC (American Type Culture Collection, Manassas, VA, USA). The cells were maintained in RPMI-1640 medium (WELGENE, Daegu, Korea) supplemented with 10% FBS (fetal bovine serum, GIBCO, Grand Island, NY, USA) and 100 mg/ml penicillin–streptomycin (WELGENE) at 37°C in a 5% $CO_2$ incubator.

Cells were plated on 60-mm plates at 60% density were treated with the drugs. The reagents used in this study including: Erlotinib (Selleckchem, Seoul, Korea). The dilutions of all agents were dissolute in DMSO (Sigma-Aldrich, MO, USA).

### *3. Transfection*

Cells were transiently transfected with the target siRNA using Lipofectamine® RNAiMAX reagent (Thermo Fisher Scientific, Waltham, MA, USA) following the manufacturer's instructions. *RSK4*, *PUMA*, and *p65* targeting siRNAs and negative control siRNAs were obtained from Bioneer (Seoul, Korea). The siRNA sequence against *RSK4*, *PUMA* and *p65* used in this study was as follows. *siRSK4*: 5'-CUG CUU UUG UUG AUA CGA A-3', *siPUMA*: 5'-ACG AGC GGC GGA GAC AAG AGG AGC AUU-3', *sip65*: 5'-ATA TGA CTT CAA GAG CAT CAT G-3'.

### *4. Trypan blue exclusion assay*

H460, H1650, HCC 827 and PC-9 cells were plated on 60-mm plates at 50% density after 24 h. Then, cells were transfected with siRNAs and harvested after 24-72 h. Cells were collected, suspended in PBS (Phosphate-Buffered Saline), and two-fold diluted with a trypan blue stain solution 0.4% (GIBCO). Twenty microliters of the mixture were placed on a hemocytometer glass (Marienfeld-Superior, Lauda-Königshofen, Germany) and analyzed using a light microscope (Olympus, Tokyo, Japan). Both viable (not stained) and non-viable (stained) cells in the hemocytometer were counted according to the manufacturer's instructions. The total cell number was calculated. Triplicate measurements were conducted for each sample.

### *5. Thiazolyl blue tetrazolium bromide (MTT) assay*

Cells were seeded as mentioned in trypan blue exclusion assay. After transfection with siRNA, cells were incubated in 60-mm plates at 37℃ for 24–72 h. Each plate was washed with PBS and incubated with 1.5 ml of reagent (MTT (Sigma-Aldrich) 1: media 9) at 37℃ for 4 h, followed by 25 min incubation with dimethyl sulfoxide. Cellular viability was quantified by measuring the absorbance at 595 nm with a PERKinElmer detector (PERKinElmer, MA, USA). Three independent experiments were performed.

### *6. Quantitative real-time PCR*

Total RNAs were extracted using TRIzol® (Invitrogen, Carlsbad, CA, USA), and 1 μg of total RNA was reversed transcribed using the AccuPower® RT PreMix (Bioneer, Daejeon, Korea). Quantitative real-time PCR was conducted using SYBR™ Select Master Mix (Thermo Fisher Scientific) according to the manufacturer's instructions. The housekeeping gene *GAPDH* was used as an internal control to normalize the variability in expression levels. The sequences of primers used in this experiment are listed in Table 1. Independent triplicates were performed.

### *7. Western blot assay*

Cells were lysed in RIPA buffer (radioimmunoprecipitation assay) (T&I, Kangwon, Korea) containing protease and phosphatase inhibitor cocktails (Sigma-Aldric) on ice for 30 min, then centrifuged at 13,000 rpm for 25 min at 4℃ to collect the supernatants. Protein concentrations were measured using the bradford assay (Bio-Rad, Hercules, CA, USA). Samples were then mixed with loading buffer and boiled at 100℃. Afterward, the samples were separated using SDS-PAGE (sodium

dodecyl sulfate-polyacrylamide gel electrophoresis) and transferred to PVDF (polyvinylidene difluoride) membranes for incubation with primary antibodies. The information of antibodies used in this experiment are listed in Table 2. Then, the membranes were incubated with horseradish peroxidase-conjugated secondary antibodies (Santa Cruz Biotechnology, CA, USA) at 24℃ for 1 h. Protein bands were detected using an enhanced chemiluminescence western blotting detection kit (Amersham, Little Chalfont, Buckinghamshire, UK).

### *8. Annexin V/PI staining assay*

Cells ($1.5 \times 10^5$ cells/well) were seeded in a 6-well plates (SPL, Pocheon-si, Korea). After transfection with siRNA and incubation for 72 h, the cells were harvested, washed with PBS, resuspended in 500 μl 1X binding buffer, and stained with 3 μl annexin V FITC and 5 μl of propidium iodide. Cells were then incubated in the dark at 24℃ for 15 min and analyzed by flow cytometry (BD Biosciences, San Joes, CA, USA).

### *9. Immunofluorescence assay*

Cells ($2 \times 10^4$ cells/well) were seeded in confocal plates (SPL). After transfection with siRNA and incubation for 8 h, the cells were fixed with methanol for 15 min under 24°C, permeabilized with 0.1% triton X-100 for 10 min, and blocked in 1% BSA (Sigma-Aldrich) for 1 h at 24°C. Next, the cells were subjected to overnight incubation with the primary antibody at 4°C. After washing three times in PBS, the cells were incubated with secondary antibodies for another 1 h at 24°C in the dark. The information of antibodies used in this experiment are listed in Table 3. Subsequent to washing in PBS, cell nucleic were separately counterstained with DAPI (VECTASHIELD, California, USA) for immunofluorescence within 5 min. Detection was then performed using a fluorescence microscope (ZEISS, LSM710, Baden-Württemberg, Germany), and the images were analyzed with ZEN (Carl Zeiss Co. Ltd, Seoul, Korea).

### *10. Statistical analysis*

All the results are presented as means ± standard deviations, and each experiment was repeated at least three times. All statistical analyses were performed using two-tailed Student's *t*-tests to determine the significance of the differences, and $p < 0.05$ was considered statistically significant.

# RESULTS

***1. RSK4 is highly expressed in lung cancer.***

Through the public online tool GEO2R analysis, I extracted 285 significant differentially expressed genes (DEGs) in the mtEGFR NSCLC patient group from GSE135164. Results showed that five up-regulated genes related to mtEGFR of NSCLC patients, including *MT1E, TINCR, RSK4, ZNF626,* and *RNF222*. Among the identified candidate genes, I focused on RSK4, associated with EGFR signaling whose role in NSCLC with mtEGFR had not been investigated previously (Figure 1A). First, to compare the expression of RSK4 in normal lung and cancer tissues, the levels of RSK4 expression in lung cancer tissues obtained from the Asan Medical Center (Seoul, Republic of Korea) were investigated. RSK4 showed higher protein expression in cancer tissues compared to normal tissues by western blot assay (Figure 1B). Subsequently, the protein levels of RSK4 in NSCLC were confirmed, and RSK4 expression was found to be high in mtEGFR (H1650, HCC 827, and PC-9 with *exon 19* deletion). However, its expression in wtEGFR cells was confirmed only in H460. RSK4 expression was not observed in H292 and H1299 (Figure 1C). Next, cells were transfected with *siRSK4* to investigate the functional association of RSK4 with mtEGFR in NSCLC. Cell death was confirmed by selecting cell lines with high RSK4 expression. Then, knockdown efficiency was confirmed by western blot assay. To measure cell death resulting from the inhibition of RSK4, trypan blue exclusion was performed. Then, cells were categorized based on cell death. The results showed that knockdown of RSK4 significantly increased cell death in mtEGFR (H1650, HCC 827 and PC-9) compared with that in wtEGFR (H460) (Figure 1D). Erlotinib is a standard treatment for patients with lung cancer targeting mtEGFR (*exon19* deletion and *exon 21 L858R*) [33]. To confirm whether mtEGFR affected RSK4 expression, I examined the effects of erlotinib on NSCLC cells. Regarding mtEGFR, the expression of RSK4 was decreased by erlotinib. These results suggest that RSK4 has specific activity mtEGFR (Figure 1E). Thus, RSK4 is highly expressed in mtEGFR and induces cell death when inhibited.

***2. RSK4 knockdown results to apoptosis in mtEGFR.***

To understand the effect of RSK4 on cell viability in mtEGFR, I transfected *siRSK4* into H460 and PC-9. Cell viability was measured after 48 h using an MTT assay. Results showed that the knockdown of RSK4 reduced the viability of PC-9 in a time-dependent manner. However, the viability of H460 did not decrease significantly (Figure 2A). Next, I investigated the expression of cleaved-caspase-3/9 to confirm the effect of RSK4 knockdown on apoptosis. Caspase-3/9 is known as a crucial marker of apoptosis that cleaves various cellular substrates [34]. Knockdown of RSK4 in PC-9 increased the expression of cleaved-caspase-3/9 in western blot assay (Figure 2B). In addition, it was confirmed that

the expression of cleaved-caspase-3 increased with RSK4 inhibition in immunofluorescence. This result was similar to the western blot assay (Figure 2C). Next, annexin V/PI double staining and flow cytometer analysis were performed to detect apoptosis. According to the knockdown of RSK4, the population of annexin V/PI-positive cells in PC-9 increased (Figure 2D). Thus, RSK4 knockdown induces apoptosis in mtEGFR cell lines.

***3. RSK4 inhibition induces apoptosis through Akt/PUMA signaling.***

Regulation of PI3K/Akt signaling in lung cancer affects sensitivity to EGFR inhibitors. In lung cancer, both Akt and ERK signaling are exclusively controlled by EGFR, and both pathways are blocked after treatment with EGFR-TKIs. However, when resistance to EGFR-TKIs occurs, the ERK signal is still downregulated, but the Akt signal is reactivated [35]. To analyze the mechanism of apoptosis in PC-9, the expression of p-Akt was confirmed by western blot assay. RSK4 Knockdown decreased p-Akt expression and increased PUMA expression (Figure 3A). It has been reported that inhibiting p-Akt in lung cancer leads to apoptosis by upregulating PUMA and BIM, which are known as BH3-only proteins [36, 41]. Therefore, I confirmed the effect of RSK4 knockdown on the mRNA and protein levels of BH3-only protein using RT-qPCR and western blot assay. Interestingly, the knockdown of RSK4 did not change the expression of BIM and BID in H460 and PC-9, but only the expression of PUMA was upregulated in PC-9 (Figure 3B-C). In addition, knockdown of RSK4 resulted in the downregulation of MCL-1, a member of the BCL-2 family (Supplementary Figure 2A). To confirm the effect of PUMA on cell death *siPUMA* and *siRSK4* were co-transfected into PC-9. Then, *siPUMA* recovered cell death induced by RSK4 knockdown (Figure 3D). To further verify this, flow cytometry analysis was performed. As a result, it was confirmed that apoptosis was recovered (Figure 3E). Thus, confirmed that *PUMA* is a major factor that induces PC-9 apoptosis at the transcriptional level.

***4. Depletion of RSK4 activates p65 translocation into the nucleus.***

I confirmed that the *PUMA* mRNA levels increased when RSK4 was knockdown. Therefore, the transcription factors that regulate *PUMA* were investigated. As a result, it was confirmed that p53 and p65 regulate the transcription level of *PUMA* [37]. First, I confirmed the expression of p-p53, which is generally known to regulate *PUMA*. However, the p-p53 expression was not changed by RSK4 knockdown (Supplementary Figure 3A). There is a p65 binding site in the *PUMA* promoter region, and when *PUMA* and p65 bind, apoptosis is induced [37-40]. Thus, I confirmed the expression of p65 by RSK4 inhibition and found that the expression of p-p65 increased in a time-dependent manner in PC-9. In addition, PUMA was the most upregulated 24 h after RSK4 inhibition (Figure 4A-B). Activation of p65 is characterized by phosphorylation of p65 and translocation to the nucleus where it activates

the transcription of target genes [40]. Therefore, to confirm the nuclear translocation of p65, I performed immunofluorescence. After 24h, p65 had been translocated from the cytosol to the nucleus in PC-9 (Figure 4C). Next, *sip65* and *siRSK4* were co-transfected to confirm the effect of p65 on cell death. Knockdown of p65 recovered cell death by RSK4 inhibition, which showed that apoptosis was recovered in flow cytometry analysis (Figure 4D-E). Thus, RSK4 knockdown in PC-9 caused p65 translocation into the nucleus and regulated PUMA transcriptional.

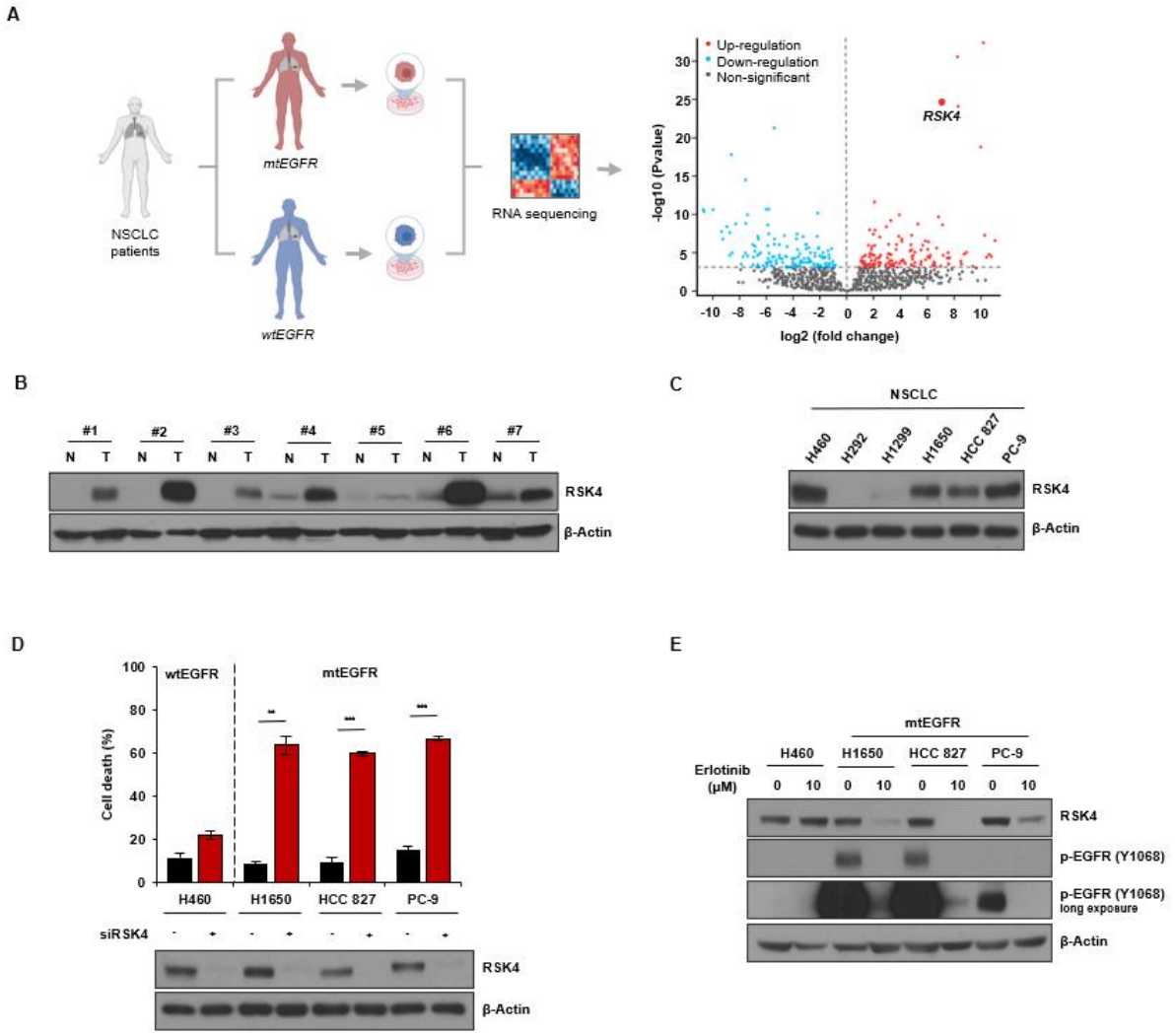


**Figure 1. Upregulated expression of RSK4 in lung cancer tissues and cell lines.** (A) Volcano plots of DEGs identified from datasets GSE135164. (B) Expression of RSK4 in lung cancer tissue patients. (C) Expression of RSK4 in NSCLC cell lines. (D) Western blot assay was performed to confirm the efficiency of transfection in NSCLC. Cell numbers were determined by trypan blue exclusion assay after 48 h. (E) NSCLC cell lines treated with DMSO or erlotinib 10 μM for 48 h, followed by western blot assay to analyze RSK4 and phosphorylated EGFR protein level. (EGFR wild type; wtEGFR, EGFR mutation type; mtEGFR). **, $p < 0.01$ and ***, $p < 0.001$ indicate the statistically significant differences from the values obtained for the control (normal) group.

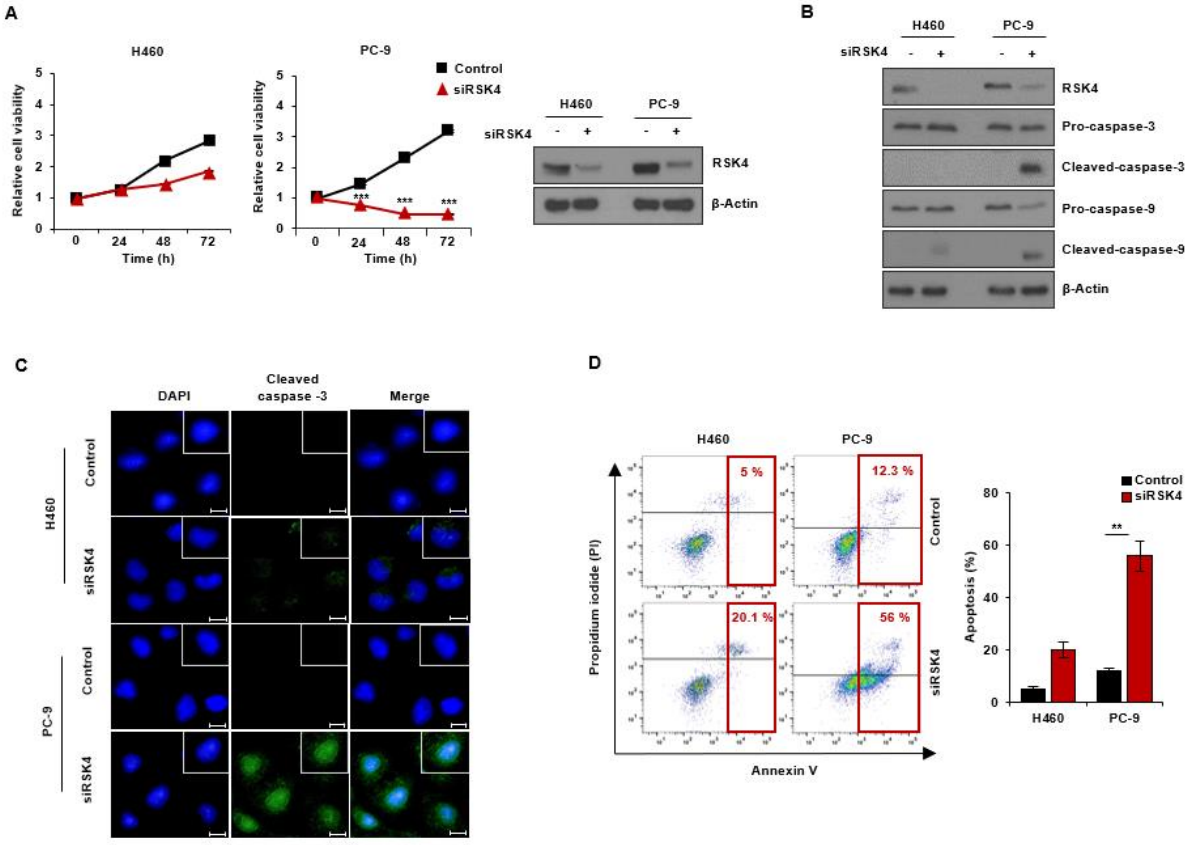


**Figure 2. Inhibition of RSK4 promotes apoptosis in mtEGFR.** (A) MTT assay in H460 and PC-9 cell lines after 48 h. Western blot assay was performed to confirm the efficiency of transfection. (B) H460 and PC-9 were transfected with *siRSK4* for 48 h. The pro-caspase-3, cleaved-caspase-3, pro-caspase-9, and cleaved-caspase-9 were detected by western blot assay. (C) The immunofluorescence assay was performed with cleaved-caspase-3 antibody (green). 4′,6-diamidino-2-phenylindole (DAPI) was used to label the nuclear (blue). The images were captured by confocal microscopy (scale bar = 20 μm). (D) H460 and PC-9 were transfected with *siRSK4* for 72 h and then analyzed for apoptosis using annexin V/PI staining assays. The data averages for each time point were calculated using the results from three independent experiments. **, $p < 0.01$ and ***, $p < 0.001$ indicate the statistically significant differences from the values obtained for the control (normal) group.

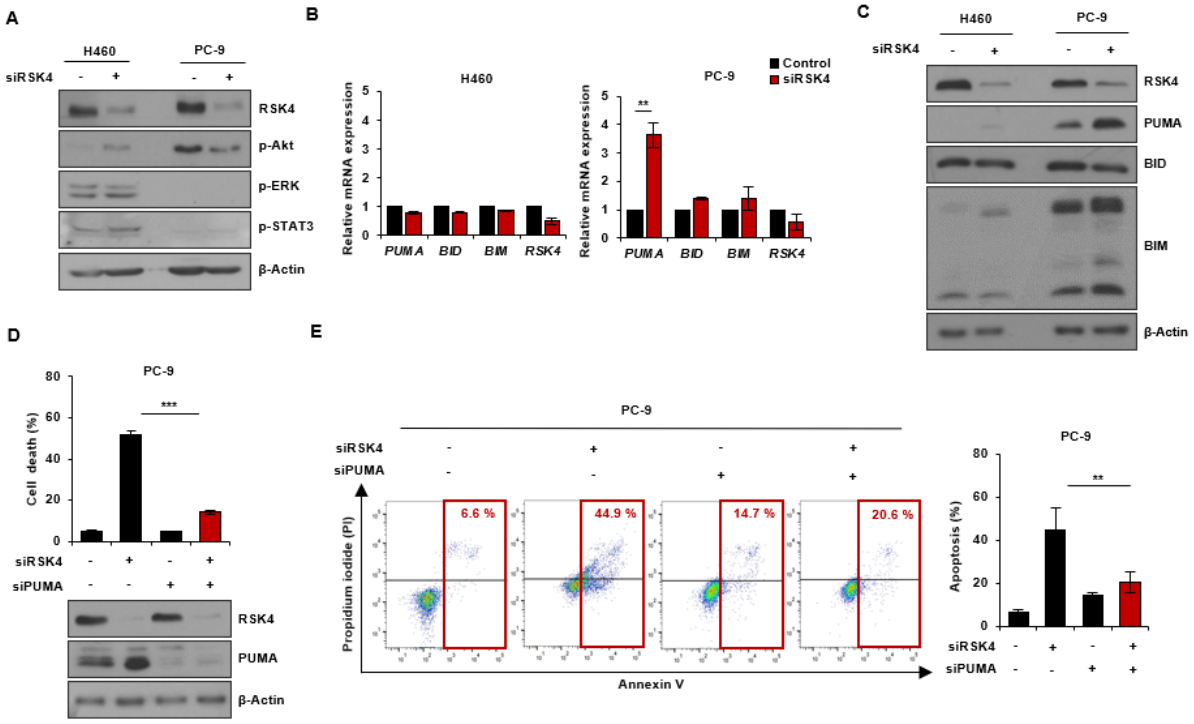


**Figure 3. Upregulation of PUMA by RSK4 knockdown induces apoptosis.** (A) H460 and PC-9 were transfected with *siRSK4* for 48 h. The p-Akt, and Akt were detected by western blot assay. (B) Relative mRNA levels of BH3-only protein target genes (*PUMA*, *BID*, and *BIM*) measured by real-time PCR. *GAPDH* was used as a standard. (C) H460 and PC-9 were transfected with *siRSK4* for 48 h. The PUMA, BIM and BID were detected by western blot assay. (D) Western blot assay was performed to confirm the transfection efficiency of *siRSK4* and *siPUMA* in PC-9 cells. Cell numbers were determined by trypan blue exclusion assay after 48 h. (E) PC-9 were transfected with *siRSK4* and *siPUMA* for 72 h and then analyzed for apoptosis using annexin V/PI staining assays. The data averages for each time point were calculated using the results from three independent experiments. **, $p < 0.01$ and ***, $p < 0.001$ indicate the statistically significant differences from the values obtained for the control (normal) group.

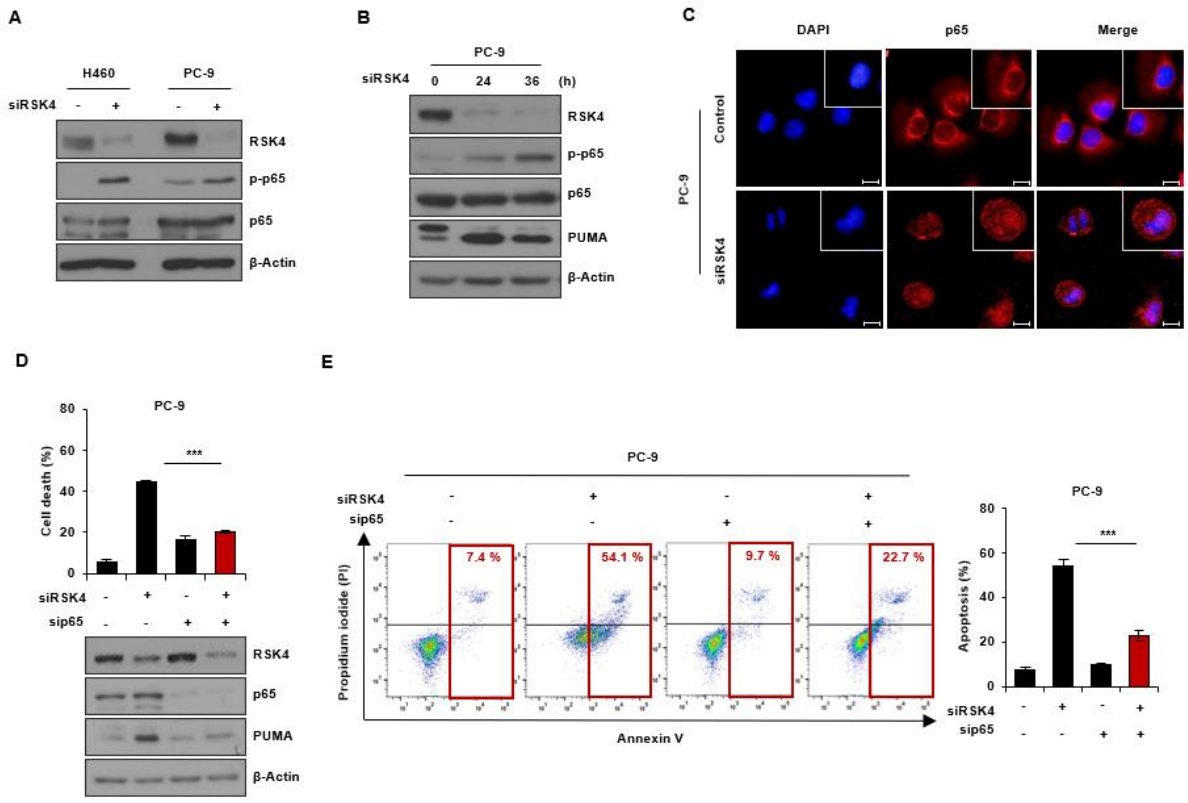


**Figure 4. Downregulation of RSK4 induces p65 phosphorylation and translocation to the nucleus.** (A) H460 and PC-9 were transfected with *siRSK4* for 48 h. The p-p65, and p65 were detected by western blot assay. (B) After transfection with *siRSK4* in PC-9, harvest was performed at 0 h, 24 h, and 36 h. Expression of p-p65 and PUMA detected by western blot assay. (C) The immunofluorescence assay was performed with a p65 antibody (red). 4′,6-diamidino-2-phenylindole (DAPI) was used to label the nuclear (blue). The images were captured by confocal microscopy (scale bar = 20 μm). (D) Western blot assay was performed to confirm the transfection efficiency of *siRSK4* and *sip65* in PC-9 cells. Cell numbers were determined by trypan blue exclusion assay after 48 h. (E) PC-9 were transfected with *siRSK4* and *sip65* for 72 h and then analyzed for apoptosis using annexin V/PI staining assays. The data averages for each time point were calculated using the results from three independent experiments. ***, $p < 0.001$ indicate the statistically significant differences from the values obtained for the control (normal) group.

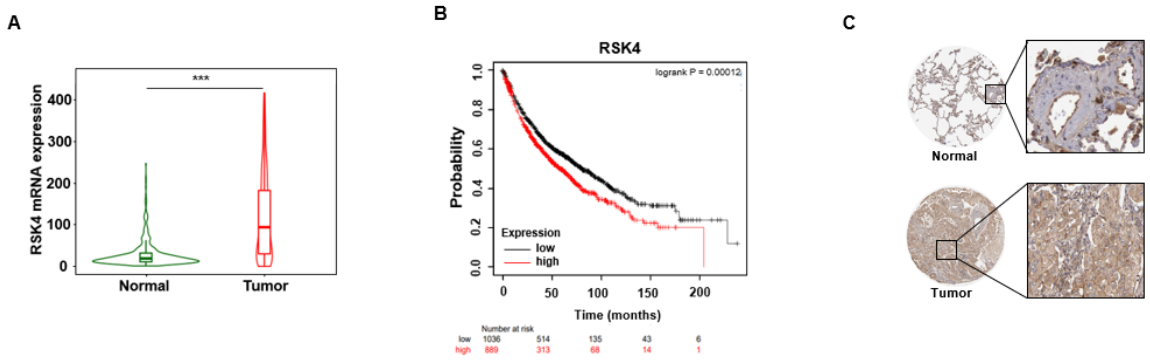


**Supplementary Figure 1.** (A) Expression profile of RSK4 in LUAD based on the TNMplot (tumor, normal, and metastatic tissues plot) database. (B) Overall survival of RSK4 in lung cancer based on the Kaplan-Meier Plotter database. (C) Expression profile of RSK4 in lung cancer tissue based on the Human Protein Atlas database. ***, $p < 0.001$ indicate the statistically significant differences from the values obtained for the control (normal) group.

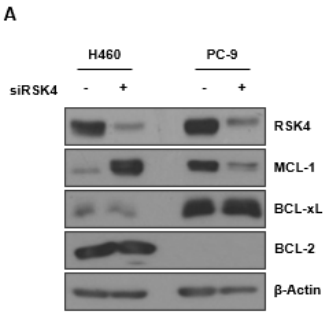


**Supplementary Figure 2.** (A) H460 and PC-9 were transfected with *siRSK4* for 48 h. The MCL-1, BCL-xL and BCL-2 were detected by western blot assay.

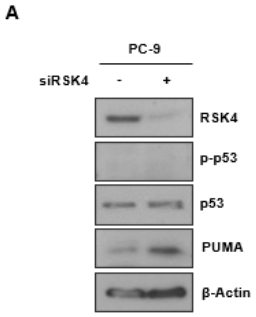


**Supplementary Figure 3.** (A) PC-9 was transfected with *siRSK4* for 48 h. The p-p53 and p53 were detected by western blot assay.

**Table 1.** List of quantitative real-time PCR primer sequences.

| Gene | | Primer sequences (5' – 3') |
|---|---|---|
| *RSK4* | Sense | CCT CCT TTC AAA CCT GCT TCT GG |
| | Anti-sense | GCT GAT GAG CAT TTG CAC TGG C |
| *PUMA* | Sense | CCT GGA GGG TCC TGT ACA ATC T |
| | Anti-sense | TCT GTG GCC CCT GGG TAA G |
| *BID* | Sense | TGA GGT CAA CAA CGG TTC CA |
| | Anti-sense | GGA AGC CAA ACA CCA GTA GGT T |
| *BIM* | Sense | CAA GAG TTG CGG CGT ATT GGA G |
| | Anti-sense | ACA CCA GGC GGA CAA TGT AAC G |

**Table 2**. List of western blot assay antibodies.

| Protein | Company | Cat. No. |
|---|---|---|
| RSK4 | Abcam | ab76117 |
| PUMA | Cell Signaling | 4976s |
| p-p65 | Cell Signaling | 3033s |
| p65 | Cell Signaling | 8242s |
| BIM | Cell Signaling | 2819 |
| BID | Cell Signaling | 2002s |
| Caspase-3 | Cell Signaling | 9662s |
| Caspase-9 | Cell Signaling | 9502s |
| p-Akt | Cell Signaling | 4060s |
| Akt | Cell Signaling | 9272s |
| p-EGFR (Y1068) | Cell Signaling | 2234 |
| p-p53 | Cell Signaling | 9284s |
| p53 | Santa Cruz | sc-126 |
| MCL-1 | Cell Signaling | 4572s |
| BCL-xL | Cell Signaling | 2764s |
| BCL-2 | Cell Signaling | 2870s |
| β-Actin | Santa Cruz | sc-47778 |

**Table 3**. List of immunofluorescence assay antibodies.

| Protein | Company | Cat. No. |
|---|---|---|
| p65 | Cell Signaling | 8242s |
| Cleaved-caspase-3 | Cell Signaling | #9664 |

# DISCUSSION

Lung cancer is the leading cause of cancer-related deaths worldwide, accounting for approximately 18% of all cancer deaths [1-2]. The overall five-year survival rate of lung cancer is only 4-17%, and the prognosis of patients with different clinical stages is significantly different. The treatment options for lung cancer include surgery, chemotherapy, radiation therapy, targeted therapy, and immunotherapy [2]. The choice of treatment depends on various factors, including the cancer stage and the presence of specific genetic mutations. Targeted therapies target EGFR mutations, which are the most frequently occurring mutations in lung cancer. Thus, EGFR-TKIs that specifically target EGFR mutations have emerged [3-5]. Although the EGFR-TKI treatment response rate is 79.3%, the limitations is that drug-resistant mutations such as EGFR *exon 19 T790M* and *exon 20 C797S* occur several months after treatment [41]. Therefore, in this study, RSK4 was presented as a new therapeutic target for NSCLC patients.

RSK4 has been reported to function as a tumor-suppressor and oncogene in various cancers [15]. While RSK1-3 are widely expressed in tissues, RSK4 differs from other RSK families in that it shows limited expression during embryonic development and has a unique activation mechanism [17-19]. Through big data analysis, I confirmed that RSK4 mRNA and protein expression increased in lung cancer (Supplementary Figure 1A-C). Additionally, RSK4 showed high expression in NSCLC patients with EGFR mutations based on GEO data analysis (Figure 1A). Therefore, we hypothesized that RSK4 has potential as a targeted therapy for NSCLC patients.

First, I demonstrated that RSK4 was highly expressed in lung cancer tissues, especially in NSCLC with mtEGFR, and confirmed that apoptosis was increased by RSK4 inhibition (Figure 1A-D). In addition, erlotinib (a first-generation EGFR-TKI) reduced RSK4 expression in mtEGFR, suggesting a potential correlation between EGFR signaling and RSK4 (Figure 1E). It was confirmed that knockdown of RSK4 induces apoptosis in mtEGFR. Apoptosis was evidenced by increased expression of cleaved caspase-3/9 (Figure 2A-C). This expression was specific to mtEGFR and was not detected in wtEGFR. These results were confirmed by annexin V/PI staining (Figure 2D). Therefore, it can be confirmed that RSK4 is an important factor for cell survival in mtEGFR. Next, I investigated the mechanism by which RSK4 affected the survival of mtEGFR. RSK4 inhibition decreased Akt phosphorylation and increased the expression of PUMA, a BH3-only protein (Figure 3A-C). In addition, I was confirmed that PUMA is a major factor that induces apoptosis by demonstrating that apoptosis was recovered through the co-transfection of *siRSK4* and *siPUMA* (Figure 3D-E). It has been reported that p65 expression in NSCLC contributes to tumor growth and binds to the PUMA promoters in colon cancer [40-41]. As the expression of PUMA was increased at the transcriptional level, I confirmed the expression of p65, a

known transcription factor (Figure 3B, 4A). Then, it was confirmed that the expression of p-p65 and PUMA were simultaneously increased by RSK4 inhibition (Figure 4B). Subsequently, using immunofluorescence, I confirmed that the nuclear translocation of p65 was induced by RSK4 knockdown (Figure 4C). Then, I found that cell death was recovered by co-transfection with *siRSK4* and *sip65* (Figure 4D-E). These results confirmed that RSK4 contributes to cell survival by regulating the expression of Akt, p65, and PUMA.

This is the first study to investigate the cellular function of RSK4 in NSCLC with mtEGFR. Thus, RSK4 is highly expressed in NSCLC with EGFR mutation and regulates progression via the Akt/p65/PUMA signaling pathway. However, the relationship between PUMA and p65 in mtEGFR should be more confirmed.

# CONCLUSION

In summary, the expression of RSK4 was upregulated in NSCLC with EGFR mutation. Accordingly, when RSK4 knockdown was in NSCLC cells harboring EGFR mutations apoptosis was induced. Mechanistically, these effects were mediated by the regulation of the Akt/p65/PUMA signaling pathway by RSK4 knockdown.

Currently, the most critical problem in NSCLC with EGFR mutation is drug resistance to generational EGFR-TKIs. EGFR-TKI drugs approved by FDA (the Food and Drug Administration) include Erlotinib, Gefitinib, Afatinib, and Osimertinib. A fourth-generation EGFR-TKI have been studied to overcome the resistance to third-generation drugs. Given that RSK4 is highly expressed in NSCLC with EGFR mutation, I propose RSK4 as a novel therapeutic target for patients with NSCLC.

# REFERENCES


1. Rahal, Z., El Nemr, S., Sinjab, A., Chami, H., Tfayli, A., & Kadara, H. (2017). Smoking and lung cancer: a geo-regional perspective. *Frontiers in oncology*, 7, 194.

2. Hirsch, F. R., Scagliotti, G. V., Mulshine, J. L., Kwon, R., Curran, W. J., Wu, Y. L., & Paz-Ares, L. (2017). Lung cancer: current therapies and new targeted treatments. *The Lancet*, *389*(10066), 299-311.

3. Xi, K. X., Zhang, X. W., Yu, X. Y., Wang, W. D., Xi, K. X., Chen, Y. Q., ... & Zhang, L. J. (2018). The role of plasma miRNAs in the diagnosis of pulmonary nodules. *Journal of Thoracic Disease*, *10*(7), 4032

4. Zarogoulidis, K., Zarogoulidis, P., Darwiche, K., Boutsikou, E., Machairiotis, N., Tsakiridis, K., ... & Spyratos, D. (2013). Treatment of non-small cell lung cancer (NSCLC). *Journal of thoracic disease*, *5*(Suppl 4), S389.

5. Jin G, Kim MJ, Jeon H-S, Choi JE, Kim DS, Lee EB, et al. PTEN mutations and relationship to EGFR, ERBB2, KRAS, and TP53 mutations in non-small cell lung cancers. Lung Cancer. 2010; 69:279–83.

6. Harrison, P. T., Vyse, S., & Huang, P. H. (2020, April). Rare epidermal growth factor receptor (EGFR) mutations in non-small cell lung cancer. In Seminars in cancer biology (Vol. 61, pp. 167-179). Academic Press

7. Wang, Q., Yang, S., Wang, K., & Sun, S. Y. (2019). MET inhibitors for targeted therapy of EGFR-TKI-resistant lung cancer. *Journal of hematology & oncology*, *12*(1), 1-11.

8. Steins, M., Thomas, M., & Geißler, M. (2014). Erlotinib. *Small Molecules in Oncology*, 109-123.

9. Wu, S. G., & Shih, J. Y. (2018). Management of acquired resistance to EGFR-TKI–targeted therapy in advanced non-small cell lung cancer. *Molecular cancer*, *17*, 1-14.

10. Miller, M., & Hanna, N. (2021). Advances in systemic therapy for non-small cell lung cancer. Bmj , 375

11. He, J., Huang, Z., Han, L., Gong, Y., & Xie, C. (2021). Mechanisms and management of 3rd-generation EGFR-TKI resistance in advanced non-small cell lung cancer. International journal of oncology, 59 (5), 1-20

12. Mansour, M. A., AboulMagd, A. M., Abbas, S. H., Abdel-Rahman, H. M., & Abdel-Aziz, M. (2023).

Insights into fourth generation selective inhibitors of (C797S) EGFR mutation combating non-small cell lung cancer resistance: a critical review. RSC advances, 3 (27), 18825-18853.

13. Fu, K., Xie, F., Wang, F., & Fu, L. (2022). Therapeutic strategies for EGFR-mutated non-small cell lung cancer patients with osimertinib resistance. Journal of Hematology & Oncology, 15 (1), 1-32.

14. Molina, N. D. R. S. D. (2019). JR. Non-Small Cell Lung Cancer: Epidemiology, Screening, Diagnosis, and Treatment [Internet]. Mayo Clin. Proc. Elsevier Ltd, 1623-1640.

15. Chen, L., Xu, T., Jia, Q., Wang, X., Li, M., & Liang, G. (2020). RSK4: a new prognostic factor in glioma. *Pathology-Research and Practice*, *216*(8), 153020.

16. Mei, Y., Liao, X., Zhu, L., & Yang, H. (2020). Overexpression of RSK4 reverses doxorubicin resistance in human breast cancer cells via PI3K/AKT signaling pathway. The Journal of Biochemistry, 167(6), 603-611.

17. Dümmler, B. A., Hauge, C., Silber, J., Yntema, H. G., Kruse, L. S., Kofoed, B., Hemmings, B. A., Alessi, D. R., & Frödin, M. (2005). Functional Characterization of Human RSK4, a New 90-kDa Ribosomal S6 Kinase, Reveals Constitutive Activation in Most Cell Types. *Journal of Biological Chemistry*, *280*(14), 13304-13314.

18. Romeo, Y., Zhang, X., & Roux, P. P. (2012). Regulation and function of the RSK family of protein kinases. Biochemical Journal, 441 (2), 553-569.

19. Xu, J., Jia, Q., Zhang, Y., Yuan, Y., Xu, T., Yu, K., Chai, J., Wang, K., Chen, L., Xiao, T., & Li, M. (2021). Prominent roles of ribosomal S6 kinase 4 (RSK4) in cancer. Pathology - Research and Practice, 219, 153374.

20. Dewdney, S. B., Rimel, B. J., Thaker, P. H., Thompson Jr, D. M., Schmidt, A., Huettner, P., ... & Goodfellow, P. J. (2011). Aberrant methylation of the X-linked ribosomal S6 kinase RPS6KA6 (RSK4) in endometrial cancers. Clinical Cancer Research, 17 (8), 2120-2129

21. Cai, J., Ma, H., Huang, F., Zhao, L., Yang, Y., Bi, J., & Zhang, T. (2014). Low expression of RSK4 predicts poor prognosis in patients with colorectal cancer. International journal of clinical and experimental pathology, 7 (8), 4959.

22. Arechavaleta-Velasco, F., Zeferino-Toquero, M., Estrada-Moscoso, I., Imani-Razavi, F. S., Olivares, A., Perez-Juarez, C. E., & Diaz-Cueto, L. (2016). Ribosomal S6 kinase 4 (RSK4) expression in ovarian tumors and its regulation by antineoplastic drugs in ovarian cancer cell lines. Medical Oncology, 33, 1-8.

23. Bender, C., & Ullrich, A. (2012). PRKX, TTBK2 and RSK4 expression causes sunitinib resistance

in kidney carcinoma-and melanoma-cell lines. International journal of cancer, 131 (2), E45-E55.

24. Li, M. Y., Fan, L. N., Han, D. H., Yu, Z., Ma, J., Liu, Y. X., ... & Wang, Z. (2020). Ribosomal S6 protein kinase 4 promotes radioresistance in esophageal squamous cell carcinoma. The Journal of clinical investigation, 130 (8), 4301-4319.

25. M. Hajj, G. N., da Silva, F. F., de Bellis, B., Lupinacci, F. C., Bellato, H. M., Cruz, J. R., ... & Roffé, M. (2020). Aberrant expression of RSK1 characterizes high-grade gliomas with immune infiltration. Molecular oncology, 14 (1), 159-179.

26. Zhu, J., Li, Q. Y., Liu, J. L., Wei, W., Yang, H. W., & Tang, W. (2015). RSK4 knockdown promotes proliferation, migration and metastasis of human breast adenocarcinoma cells. *Oncology reports*, *34*(6), 3156-3162.

27. Thakur, A., Rahman, K. W., Wu, J., Bollig, A., Biliran, H., Lin, X., ... & Liao, J. D. (2007). Aberrant expression of X-linked genes RbAp46, Rsk4, and Cldn2 in breast cancer. Molecular cancer research, 5 (2), 171-181.

28. Li, A., Liu, D., Liu, Y., Zhou, Y., Du, Z., & Song, J. (2018). A pilot study of RSK4 expression in patients with human non-small cell lung carcinoma. Annals of Clinical & Laboratory Science, 48 (4), 484-489.

29. Fang, Y., Ma, C., Gan, L., Luo, Q., He, Q., Xie, M., Li, Y., Chen, G., Wei, M., & Hu, H. (2018). Clinicopathological significance of ribosomal protein S6 kinase A6 in lung squamous cell carcinoma: An immunohistochemical and RNA-seq study. *International Journal of Clinical and Experimental Pathology*, *11*(3), 1318-1327.

30. Sun, Y., Cao, S., Yang, M., Wu, S., Wang, Z., Lin, X., ... & Liao, D. J. (2013). Basic anatomy and tumor biology of the RPS6KA6 gene that encodes the p90 ribosomal S6 kinase 4. Oncogene, 32 (14), 1794-1810.

31. He, Q., He, R., Luo, W., Gan, X., Ma, J., Chen, G., Li, P., Lan, D., & Hu, X. (2017). Expression of RSK4 in lung adenocarcinoma tissue and its clinicopathological value: A study based on RNA-seq data and immunohistochemistry. International Journal of Clinical and Experimental Pathology, 10(12), 11405-1141

32. Chrysostomou, S., Roy, R., Prischi, F., Thamlikitkul, L., Chapman, K. L., Mufti, U., Peach, R., Ding, L., Hancock, D., Moore, C., Molina-Arcas, M., Mauri, F., Pinato, D. J., Abrahams, J. M., Ottaviani, S., Castellano, L., Giamas, G., Pascoe, J., Moonamale, D., . . . Pardo, O. E. (2021). Repurposed floxacins targeting RSK4 prevent chemoresistance and metastasis in lung and bladder cancer. Science Translational Medicine.

33. Hsu, W. H., Yang, J. H., Mok, T. S., & Loong, H. H. (2018). Overview of current systemic management of EGFR-mutant NSCLC. Annals of Oncology, 29, i3-i9.

34. Han, M. H., Park, C., Jin, C. Y., Kim, G. Y., Chang, Y. C., Moon, S. K., ... & Choi, Y. H. (2013). Apoptosis induction of human bladder cancer cells by sanguinarine through reactive oxygen species-mediated up-regulation of early growth response gene-1. PloS one, 8(5), e63425

35.Cairns, J., Fridley, B. L., Jenkins, G. D., Zhuang, Y., Yu, J., & Wang, L. (2018). Differential roles of ERRFI1 in EGFR and AKT pathway regulation affect cancer proliferation. *EMBO reports*, *19*(3), e44767.

36. Bean, G. R., Ganesan, Y. T., Dong, Y., Takeda, S., Liu, H., Chan, P. M., Huang, Y., Chodosh, L. A., Zambetti, G. P., Hsieh, D., & Cheng, Y. (2013). PUMA and BIM Are Required for Oncogene Inactivation–Induced Apoptosis.

37. Yu J, Zhang L. PUMA, a potent killer with or without p53. Oncogene. 2008; 27: S71-83.

38. Sun, L., Huang, Y., Liu, Y., Zhao, Y., He, X., Zhang, L., ... & Zhang, Y. (2018). Ipatasertib, a novel Akt inhibitor, induces transcription factor FoxO3a and NF-κB directly regulates PUMA-dependent apoptosis. Cell death & disease, 9 (9), 911.

39. Wang, P., Qiu, W., Dudgeon, C., Liu, H., Huang, C., Zambetti, G. P., ... & Zhang, L. (2009). PUMA is directly activated by NF-κB and contributes to TNF-α-induced apoptosis. Cell Death & Differentiation, 16 (9), 1192-1202.

40. Chen, D., Wei, L., Yu, J., & Zhang, L. (2014). Regorafenib inhibits colorectal tumor growth through PUMA-mediated apoptosis. Clinical cancer research, 20 (13), 3472-3484.

41. Rasmi, R. R., Sakthivel, K. M., & Guruvayoorappan, C. (2020). NF-κB inhibitors in treatment and prevention of lung cancer. *Biomedicine & Pharmacotherapy*, *130*, 110569

# 국문 요약


폐암은 전 세계적으로 암 관련 사망의 주요 원인이다. 초기에 특징적인 증상이 나타나지 않기 때문에 조기 진단이 어려우며, 진단을 받더라도 수술이 불가능한 경우가 많아 예후가 좋지 않은 것으로 보고되고 있다. 이러한 폐암의 치료 옵션에는 수술, 화학 치료, 방사선 치료, 표적 치료 및 면역 치료가 있다. 치료를 선택할 때는 병리학적 특징, 암의 병기 및 특정 유전적 돌연변이의 존재를 포함하여 다양한 요인을 고려하여 선택된다. 이 중 표적 치료는 EGFR을 표적으로 하는 EGFR-TKI를 사용하며, 약물 반응률은 79.8%로 높은 수준이지만 환자들 대부분이 수개월 후 약물에 저항성을 가지는 2차 돌연변이가 발생한다는 한계점이 있다. 이러한 한계점을 극복하고자 현재까지도 폐암에서 화학요법 및 표적 치료법에 대한 연구가 활발히 진행되고 있으나, 뚜렷한 치료법이 정립되지 않아 새로운 치료제의 개발이 필요한 실정이다.

RSK4는 p90 리보솜 단백질 S6 키나아제 중 하나로, 세린-트레오닌 키나아제에 속하며 여러 암종에서 종양 유전자 및 종양 억제자로 기능한다. GEO 데이터베이스를 통해 EGFR 야생형 대비 돌연변이를 가지는 폐암 환자군에서 유의하게 높은 발현을 보이는 상위 유전자 중 RSK4를 동정하였다. 이를 바탕으로 실제 폐암 환자 조직에서 발현을 확인한 결과, 정상 대비 폐암 조직에서 RSK4의 발현이 높은 것을 확인하여 *in silico* 데이터를 검증하였다. 이후 인간 폐암 세포주에서 RSK4 발현을 저해하였을 때, 세포 사멸이 유도되었으며 이는 EGFR 돌연변이를 가지는 폐암 세포주에서 높은 비율로 발생하였다. RSK4 억제 시 유도되는 세포 사멸은 폐암에서 중요한 신호전달 유전자로 알려진 p-Akt의 발현을 저해하며, PUMA의 mRNA 수준을 상향 조절하였다. 뿐만 아니라, PUMA 발현 저해 시 RSK4 억제로 유도된 세포 사멸이 회복되는 것을 확인하였다. 이를 통해 PUMA를 조절하는 전사인자 중, PUMA의 프로모터에 결합한다고 보고된 p65의 발현을 확인하였다. p65는 활성화 시에 표적 유전자를 조절하는 전사인자로써 보고되어 RSK4를 저해한 후, immunofluorescence 분석을 통해 p65의 위치가 세포질에서 핵 내로 전위 되는 것을 확인하였다. 종합하자면, RSK4의 억제가 Akt/p65/PUMA 신호 기전을 통해 EGFR 돌연변이를 가지는 폐암 세포주에서 세포 사멸을 일으킴을 검증하였다.

결론적으로 본 연구에서는 EGFR 돌연변이를 가지는 폐암 환자에서 RSK4 발현이 증가되어 있다는 것과 폐암 세포주에서 RSK4 억제의 항암 효능 및 분자 기전을 검증하였다. 하여, 이를 통해 EGFR 표적 치료제의 한계점을 극복하여 환자들을 위한 새롭고 잠재적

인 치료 표적으로서 RSK4의 가능성을 제시하고자 한다.